ADVANCED MULTIVARIATE INVERSION TECHNIQUES FOR HIGH RESOLUTION 3D GEOPHYSICAL MODELING

Monica Maceira[1], Haijiang Zhang[2], Carene Larmat[1], Charlotte A. Rowe[1], and Michael L. Begnaud[1]

Los Alamos National Laboratory[1] and Massachusetts Institute of Technology[2]

ABSTRACT

To meet the United States Government nuclear explosion monitoring requirements with high confidence, the Air Force Technical Applications Center needs new and improved capabilities for analyzing regional seismic, teleseismic, and infrasound event data. Recently, the National Nuclear Security Administration has decided to move toward 3D modeling to improve knowledge of the compressional and shear velocity structure and enable us to reduce uncertainty and more accurately detect, locate, and identify small (body wave magnitude $m_b<4$) seismic events. For seismically active areas, inaccurate models can be corrected using the kriging methodology and, therefore, it is possible to detect, locate, and identify large events even with limited resolution models. This is not necessarily the case for smaller events, however, and it is even more of a challenge for aseismic regions. Furthermore, interest on near-regional to local monitoring demands that we address the Earth's heterogeneities and 3D complexities.

Motivated by the shortcomings of existing single-parameter inversion methods in accurate prediction of other geophysical parameters, this research was mainly focused on the development and refinement of advanced multivariate inversion techniques to generate a realistic, comprehensive, and high-resolution 3D model of the seismic structure of the crust and upper mantle that satisfies multiple independent geophysical datasets. We present 3D seismic velocity models of the crust and upper mantle beneath three different regions (northwest China; the East Africa Rift System; and Utah) resulting from the simulatenous and joint use of seismic body wave arrival times, surface wave dispersion measurements, and gravity data. Our methodology represents a robust and consistent compromise that fits the different datasets within accepted tolerances. In addition to obtain the optimum earth model fitting the multiple observations, we showed our intial results towards an independent assessment of the prediction capability of these newly computed models using a purely numerical method for wave propagation modeling (the Spectral Element Method).

1. REPORT DATE **SEP 2011**	2. REPORT TYPE	3. DATES COVERED **00-00-2011 to 00-00-2011**
4. TITLE AND SUBTITLE **Advanced Multivariate Inversion Techniques for High Resolution 3D Geophysical Modeling**		5a. CONTRACT NUMBER
		5b. GRANT NUMBER
		5c. PROGRAM ELEMENT NUMBER
6. AUTHOR(S)		5d. PROJECT NUMBER
		5e. TASK NUMBER
		5f. WORK UNIT NUMBER
7. PERFORMING ORGANIZATION NAME(S) AND ADDRESS(ES) **Los Alamos National Laboratory,P.O. Box 1663 ,Los Alamos,NM,87545**		8. PERFORMING ORGANIZATION REPORT NUMBER
9. SPONSORING/MONITORING AGENCY NAME(S) AND ADDRESS(ES)		10. SPONSOR/MONITOR'S ACRONYM(S)
		11. SPONSOR/MONITOR'S REPORT NUMBER(S)
12. DISTRIBUTION/AVAILABILITY STATEMENT **Approved for public release; distribution unlimited**		
13. SUPPLEMENTARY NOTES **Published in the Proceedings of the 2011 Monitoring Research Review - Ground-Based Nuclear Explosion Monitoring Technologies, 13-15 September 2011, Tucson, AZ. Volume I. Sponsored by the Air Force Research Laboratory (AFRL) and the National Nuclear Security Administration (NNSA). U.S. Government or Federal Rights License**		

14. ABSTRACT

To meet the United States Government nuclear explosion monitoring requirements with high confidence, the Air Force Technical Applications Center needs new and improved capabilities for analyzing regional seismic teleseismic, and infrasound event data. Recently, the National Nuclear Security Administration has decided to move toward 3D modeling to improve knowledge of the compressional and shear velocity structure and enable us to reduce uncertainty and more accurately detect, locate, and identify small (body wave magnitude mb<4) seismic events. For seismically active areas, inaccurate models can be corrected using the kriging methodology and therefore, it is possible to detect, locate, and identify large events even with limited resolution models. This is not necessarily the case for smaller events, however, and it is even more of a challenge for aseismic regions. Furthermore, interest on near-regional to local monitoring demands that we address the Earth?s heterogeneities and 3D complexities. Motivated by the shortcomings of existing single-parameter inversion methods in accurate prediction of other geophysical parameters, this research was mainly focused on the development and refinement of advanced multivariate inversion techniques to generate a realistic, comprehensive, and high-resolution 3D model of the seismic structure of the crust and upper mantle that satisfies multiple independent geophysical datasets. We present 3D seismic velocity models of the crust and upper mantle beneath three different regions (northwest China; the East Africa Rift System; and Utah) resulting from the simulatenous and joint use of seismic body wave arrival times surface wave dispersion measurements, and gravity data. Our methodology represents a robust and consistent compromise that fits the different datasets within accepted tolerances. In addition to obtain the optimum earth model fitting the multiple observations, we showed our intial results towards an independent assessment of the prediction capability of these newly computed models using a purely numerical method for wave propagation modeling (the Spectral Element Method).

15. SUBJECT TERMS

16. SECURITY CLASSIFICATION OF:			17. LIMITATION OF ABSTRACT	18. NUMBER OF PAGES	19a. NAME OF RESPONSIBLE PERSON
a. REPORT **unclassified**	b. ABSTRACT **unclassified**	c. THIS PAGE **unclassified**	**Same as Report (SAR)**	**11**	

OBJECTIVES

The ultimate goal of this study is to improve our knowledge of the 3D compressional and shear velocity structure and enable us to reduce uncertainty and more accurately detect, locate, and identify small (body wave magnitude m_b<4) seismic events, and therefore improve our capabilities for nuclear explosion monitoring (NEM). This project specifically improves seismic monitoring technology through the development and application of advanced multivariate inversion techniques to generate a realistic, comprehensive, and high-resolution 3D model of the seismic structure of the crust and upper mantle that satisfies numerous independent geophysical datasets.

RESEARCH ACCOMPLISHED

Inversion of surface wave dispersion data is a standard method for determining 3D shear velocity structure of the crust and upper mantle of the Earth. On the one hand, inversion of phase or group velocity dispersion of surface waves excited by earthquakes (and measured at relatively low frequencies) has revealed shear wavespeed variations at wavelengths upward of 300 km (e.g., Ritzwoller and Levshin, 1998; Huang et al., 2003; Lebedev and Van der Hilst, 2008; Yi et al., 2008). On the other hand, ambient noise tomography – with surface wave Green's functions estimated from cross correlation of seismic ambient noise – has been used to image crustal Vs variation with a lateral resolution upward of 100 km either on regional or on sub-continental scales (e.g., Zheng et al., 2008; Yang et al., 2010; Yao et al., 2010). Body wave travel-time tomography and surface wave tomography each have their specific strengths and weaknesses. Travel time tomography can yield higher resolution in regions of dense path coverage, and it generally has excellent lateral resolution beneath regions of high seismic activity or dense station coverage. In regions of low seismicity and sparse station distribution, however, the shallow subsurface cannot be resolved adequately by direct P or S travel times. In contrast, surface wave data generally yield better radial resolution and have better potential for resolving shallow mantle structure beneath regions that are aseismic or which are void of seismograph stations. To benefit from the complementary sampling of different seismic datasets (such as body and surfaces waves), multivariate inversion techniques should be considered. This could be achieved by full waveform inversion (e.g., Tromp et al., 2005; Zhao and Jordan, 2006), with the implicit consideration of finite frequency kernels computed in heterogeneous media, but the huge computational cost of such an approach makes it as yet impractical for routine implementation in an operational setting. During this project and with such operational aspects in mind, we focused on approximations to full wave propagation which are computationally efficient and still sufficiently accurate for the goal of routine earthquake location and nuclear monitoring.

Gravity measurements can provide constraints on spatial variations in (mass) density of rock in the subsurface, but like any other potential field method interpretation of gravity anomalies is plagued by substantial ambiguity. Indeed, weak and broad structures in the shallow subsurface can produce the same gravity signal (at the surface) as a small, strong density anomaly at a larger depth. Using an empirical relationship between velocity and density, Maceira and Ammon (2009) combined surface wave dispersion and gravity observations into a single inversion to obtain a self-consistent high-resolution 3D shear velocity and density model with increased resolution of shallow geologic structures. For a study of Tarim Basin (western China) they used gravity data from the GRACE satellite mission (Tapley et al., 2005) along with high-resolution surface wave slowness tomographic maps (Maceira et al., 2005), and the 3D velocity model obtained from their joint inversion fits simultaneously both data sets. Encouraged by these results and motivated by the shortcomings of existing single-parameter inversion methods in accurate prediction of other geophysical parameters (e.g. Julià et al. 2000), we have developed an advanced multivariate inversion technique to generate a realistic, comprehensive, and high-resolution 3D model of the seismic structure of the crust and upper mantle that satisfies multiple independent geophysical datasets.

Our final algorithm and code JointTomoDD is a modification of the Maceira and Ammon (2009) joint inversion code, in combination with the regional version of the double-difference (DD) tomography program *tomoDD* (Zhang and Thurber, 2003, 2006), with a fast LSQR solver operating on the gridded values jointly. The model representation is a combination of columns of rectangular prisms (for gravity forward modeling) embedded in a grid whose nodes are located at the center of each prism. In a simplified manner, the system of equations to be inverted can be written in the form:

$$w_t G_t m = d_t \text{; model includes compressional and shear-wave velocities}$$

$$w_g G_g m = d_g \text{; model includes compressional and shear-wave velocities}$$

$w_s G_s m = d_s$; model includes shear-wave velocities only;

where w_t, w_g, and w_s are weighting parameters for seismic arrival times, gravity, and surface wave dispersion data respectively, that equalize the three data sets. First-order smoothing and damping are also appplied to the model. Please refer to Maceira et al. (2009) for further details.

East Africa Rift System

Knowledge of lithospheric structure is of importance for understanding East Africa's geodynamic evolution and for addressing broader questions about the causes of continental breakup. Though recent investigations have yielded improved characterizations of the rift zone, many uncertaintites remain. For example, the basalt dominated magmatism in East Africa has been explained by both one deep mantle plume (Ebinger and Sleep, 2001) and two plumes (Rogers et al., 2000). Magma-assisted rifting in the northern Main Ethiopian Rift contrasts with fault-controlled extension further south (Beutel et al., 2010), but in many cases the extent of lithospheric thinning and temporal and spatial evolution of rifting remain unclear (e.g., Ebinger, 1989). Key to resolving such issues are better constrained seismic models. We implemented JointTomoDD in this region. Benefits of our joint inversion approach appear pronounced when working with regions of strong lateral contrast as found in central Asia (Maceira and Ammon, 2009). In applying the joint inversion technique to East Africa, we solve for velocity structure in an area with less lateral heterogeneity but great tectonic complexity. To increase the effectiveness of the technique in this region we explore gravity filtering methods and test different velocity-density relations (Modrak et al, 2011).
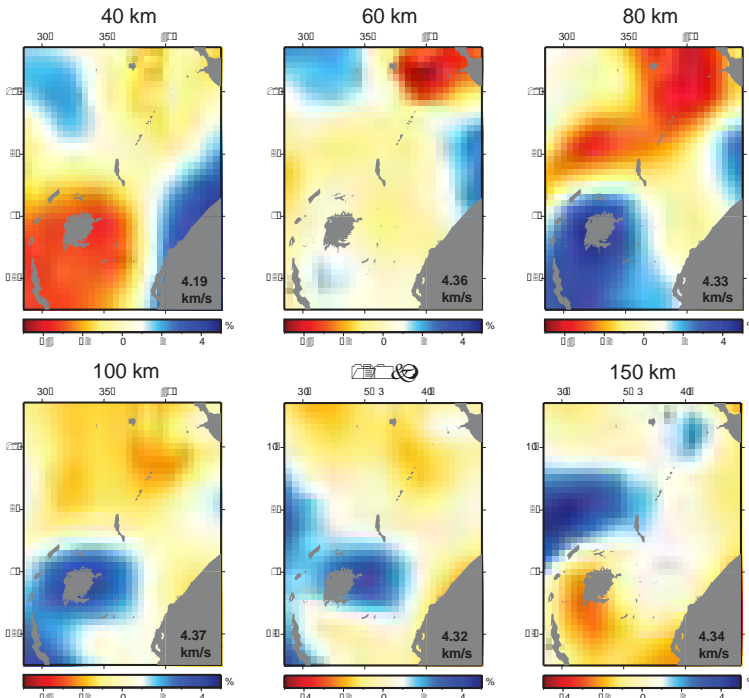

Figure 1. Horizontal δVs/Vs cross-sections at various depths through the 3D velocity model obtained from the joint inversion. Percent values are with respect to mean velocities shown in the corner of each cross-section.

The area for the inversion spans the broad uplifted region from Ethiopia at one end to Kenya, Uganda, and Tanzania at the other. Near the northern boundary of our study area, the Main Ethiopia Rift meets the incipient Red Sea and Gulf of Aden spreading ridges. At the opposite end, the rift system splits into distinct western and eastern branches, which largely sidestep the Archean Tanzania craton. Recent inversions of East Africa have employed body waves (e.g., Bastow et al., 2005; Benoit et al., 2006), surface waves (e.g., Knox et al., 1998; Weeraratne et al., 2003), receiver functions, or some combination of these (e.g., Julià et al., 2005; Keranen et al., 2009). Although useful comparisons can be drawn between the Ethiopian and Tanzanian portions of the rift system, most tomographic studies to date have focused exclusively on one section or the other. The current inversion, in contrast, is carried out over a wider area than most previous studies, allowing straightforward comparison between these two distinct portions of the rift system.

Fundamental-mode Rayleigh wave group velocity estimates with periods from 7 s to 150 s were obtained from Pasyanos and Nyblade (2007) for the inversion. Though less detailed than images from local seismic arrays (e.g., Prodehl et al., 1997), these estimates span a broader spatial and period range. Gravity data for the inversion were derived from the Gravity Recovery and Climate Experiment (GRACE) (Tapley et al., 2005). We implemented a method to increase the usefulness of gravity data by filtering the Bouguer anomaly map. Though commonly applied

in gravity forward modeling (e.g., Simiyu and Keller, 1997), such techniques have not to our knowledge been used in previous joint inversion studies (e.g., Lees and VanDecar, 1991; Zeyen and Achauer 1997; Tiberi et al., 2003). Different tests suggest that addition of unfiltered gravity data contributes little in the way of distinguishing between features at different depths. Rather than improving resolution at shallow depths as desired, features in the unfiltered gravity data are smeared into the mantle. Although filtering removes potentially useful information on mantle structure, the remaining short-wavelength signal can be assigned with greater reliability within the crust, avoiding the mutually degrading effects of smearing between crust and mantle. To remove the long-wavelength components from the Bouguer gravity map we follow Tessema and Antoine (2004), who use an upward continuation method and demonstrate correlation with crustal geology.

Figure 1 shows the 3D S-wave velocity model obtained from the joint inversion. The low-velocity anomaly beneath Ethiopia is among the most prominent features. The anomaly appears most conspicuous at ~60 km depth beneath Afar and continues southward along the Main Ethiopian Rift at greater depths. Although low velocities beneath Ethiopia appear pronounced up to ~140 km, Fig. 1 suggests the magnitude of the anomaly becomes somewhat diminished by ~150 km. Such a result appears in agreement with a number of regional surface wave studies. For example, while Ritsema and Van Heijst (2000) resolve a low-velocity anomaly beneath Ethiopia extending to at least 250 km, a decrease in the magnitude of this anomaly becomes visible at around 160 km. Similar magnitude decreases are visible in the results of Knox et al. (1998) and Pasyanos and Nyblade (2007). Besides the low-velocity anomaly below Ethiopia, prominent velocity excursions also occur below Tanzania. In the 40 km depth slice we resolve lower shear velocities beneath the Tanzania craton than in the adjoining rift branches; at this depth, lower velocities beneath the craton are readily explained by the contrast between thick crust in the craton and shallow mantle in the
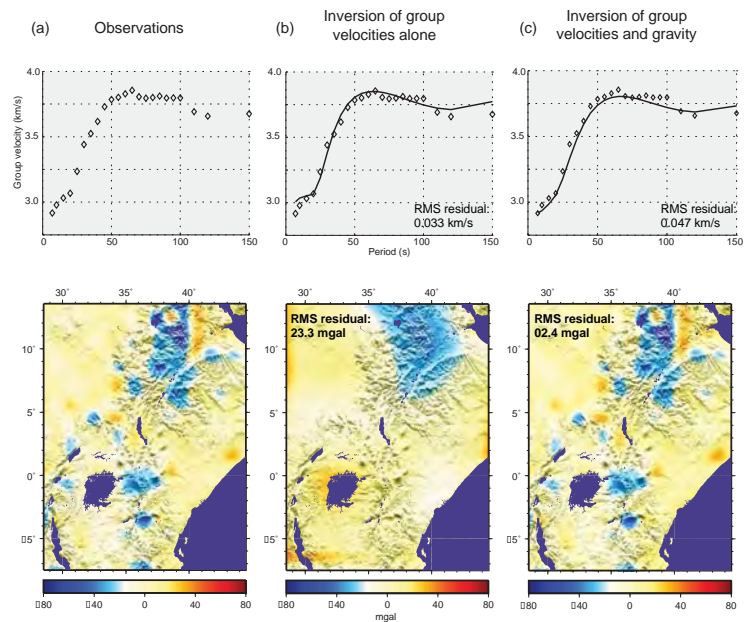

Figure 2. Fit-to-data from inversion of group velocities only and from inversion of group velocities and gravity. (a) Top: Group velocities from a representative cell in the model. Bottom: Filtered Bouguer anomalies. (b) Top: Group velocity fit obtained from inversion of group velocities only. Bottom: Gravity fit obtained from inversion of group velocities only. (c) Top: Group velocity fit obtained from joint inversion. Bottom: Gravity fit obtained from joint inversion.

surrounding rift branches. Beginning at 50 km, velocities in the craton revert to higher values than in the adjacent non-cratonic terranes; these higher values persist to ~120 km. Finally, at ~140 km, a pronounced low-velocity anomaly emerges beneath the craton. This juxtaposition of high and low shear-wave speeds between 120-140 km depth appears consistent with the hypothesis, discussed in detail by Weeraratne et al. (2003) and Nyblade et al. (2000), of a hot, upwelling plume impeded by cool, overlying material of the craton. Additionally, our results allow comparison between rift structure of Ethiopia and Tanzania. In obtaining data from Pasyanos and Nyblade (2007), we use group velocities derived not only from local stations and events, but also from stations and events distributed across surrounding tectonic plates. Though the resulting continent-scale maps possess less detail than local-scale group velocity maps, their wider spatial coverage allows straight-forward comparison between distinct portions of the rift system. As a result, we find that uppermost mantle shear velocities beneath Ethiopia appear much slower than those beneath Tanzania. While the presence of shallow low velocities beneath Ethiopia suggests that mantle lithosphere there has been largely replaced by asthenosphere (e.g., Beutel et al., 2010), the absence of shallow low velocities beneath the southern rift branches is consistent with fault-controlled extension in that part of the rift system. Finally, though a common origin at greater depths is not ruled out, no evidence is observed that the various

low-velocity anomalies in Fig. 1 merge continuously above 175 km. This possibly explains why igneous rocks from the two low velocity zones are compositionally different (e.g., Rogers et al., 2000).

In the inversion carried out in central Asia by Maceira and Ammon (2009), addition of gravity data dramatically improved the fit to the Bouguer anomalies without significantly degrading the fit to the group velocities. Figure 2 demonstrates this result for the current study area as well. Although it is well known that problems of non-uniqueness make gravity data easier to match than seismic data, several observations provide confidence in our methodology's robustness. These include the simultaneous fit to both data sets shown in Fig. 2 as well as qualitative changes resulting from the addition of gravity data. For example, compared with results from the inversion of group velocities only, the joint inversion methodology provides increased effectiveness capturing Moho depth at the continental margin and sharper delineation of the Tanzania craton. The resolved extent of the high-velocity cratonic region accords well with previous tomographic images (e.g., Fig. 11 of Weeraratne et al., 2003) as well as geodynamic models suggesting strain localization in zones of weakness surrounding the craton (e.g., Nyblade and Brazier, 2002).
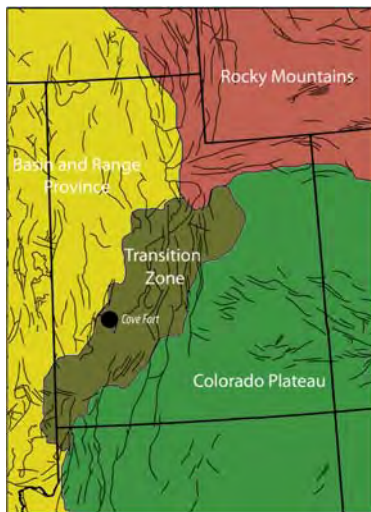
Utah Geothermal Region

Figure 3. Simplfied tectonic map showing tectonic provinces around Cove Fort geothermal field.

The Cove Fort-Sulphurdale geothermal area is located in the transition zone between the Basin and Range to the west and the Colorado Plateau to the east (Figure 3). We have collected various geophysical data around the geothermal field, including gravity anomalies (Pan-American Center for Earth and Environmental Studies (PACES) available at http://gis.utep.edu), seismic surface wave phase and group velocity maps (Yang et al., 2008), and seismic body wave arrival times that were assembled from seismic waveforms recorded by the University of Utah Seismograph Stations (UUSS) regional network for the past 7 years and the recent EArthscope/USArray phase data. Various geophysical data sets indicate that beneath the Cove Fort-Sulphurdale geothermal resource there is a strong anomaly of low seismic velocity, low gravity and high electrical conductivity that correlates with the high surface heat flow. This suggests that there is a heat source in the crust beneath the geothermal field. We collected first P arrival data from more than 6500 earthquakes in the Utah region. Each event has at least 6 arrivals for reliably determining its location. We applied the double-difference seismic tomography method (Zhang and Thurber, 2003) to simultaneously determine an initial velocity structure and earthquake locations. On the preliminary regional seismic velocity map computed this way, we can also identify some other low velocity anomalies, indicating other potential geothermal prospects. We then applied our simultaneous joint inversion methodology to produce a better constrained velocity structure of the Utah area which will be very helpful for characterizing and exploring existing and potential geothermal reservoirs in the area.
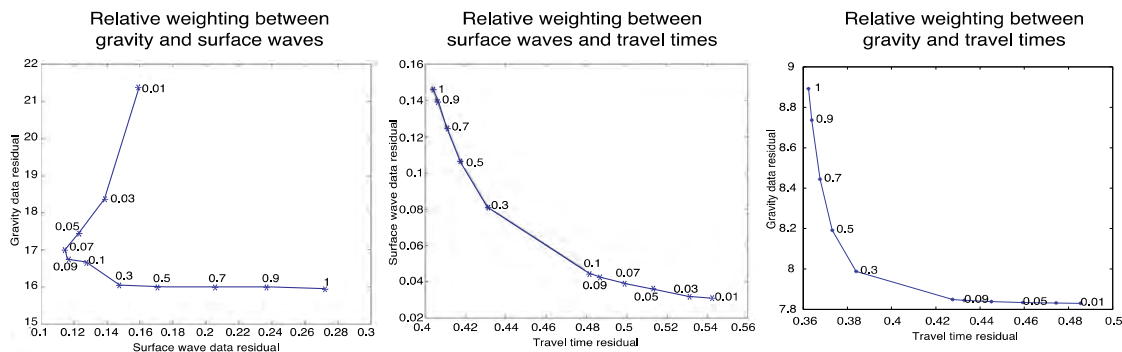

Figure 4. Trade-off curves between datasets pairs are used to decide on relative weighting.

Joint inversion of seismic travel times, surface wave dispersion, and gravity data represents a multiple-objective optimization problem. Because it is unlikely that the different "objectives" (data types) would be optimized by the same parameter choices, some trade-off between the objectives is needed. Figure 4 shows an example of finding the relative weightings between the multiple data types through a trade-off analysis of data residuals. As a result, the final model will optimally fit the different datasets.

Travel Time RMS residual: 147 ms
Gravity RMS residual: 20 mgal

Travel Time RMS residual: 189 ms
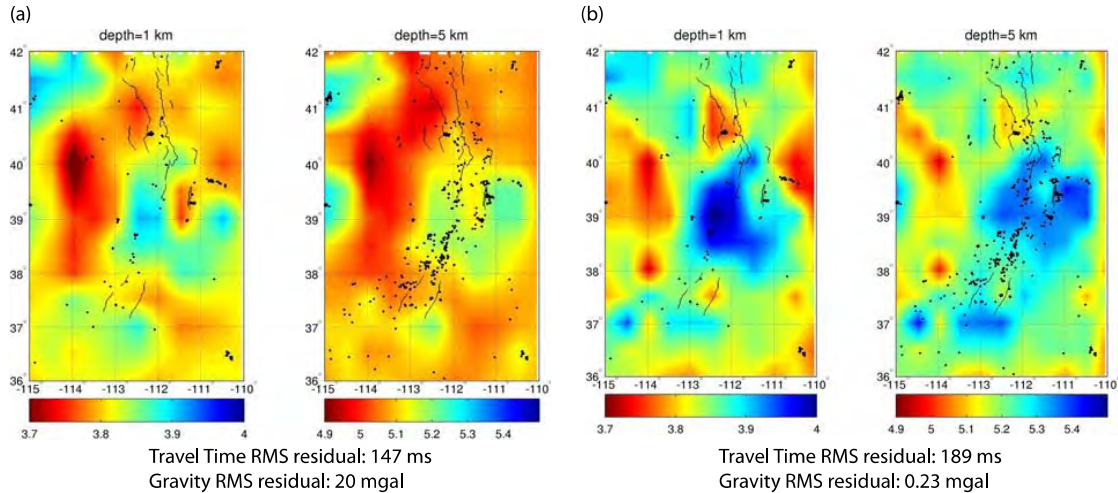Gravity RMS residual: 0.23 mgal

Figure 5. Compressional-wave velocity model at constant depth slices using (a) seismic travel times alone and (b) joint inversion of body waves travel times and gravity. (Velocity units: km/s).

Figures 5 and 6 show different depth slices through the computed model for compressional and shear-wave velocity respectively. Figure 5 shows the comparison of the Vp model obtained from travel time arrivals only with that obtained using seismic arrivals together with gravity anomaly information. Figure 6 shows the comparison of the Vs model obtained from the joint inversion of surface wave and gravity data with that obtained using all three data types. The latter model fits the three data sets well and shows better definition of the velocity anomaly associated with the transition from the Basin and Range to the west to the Colorado Plateau to the east.
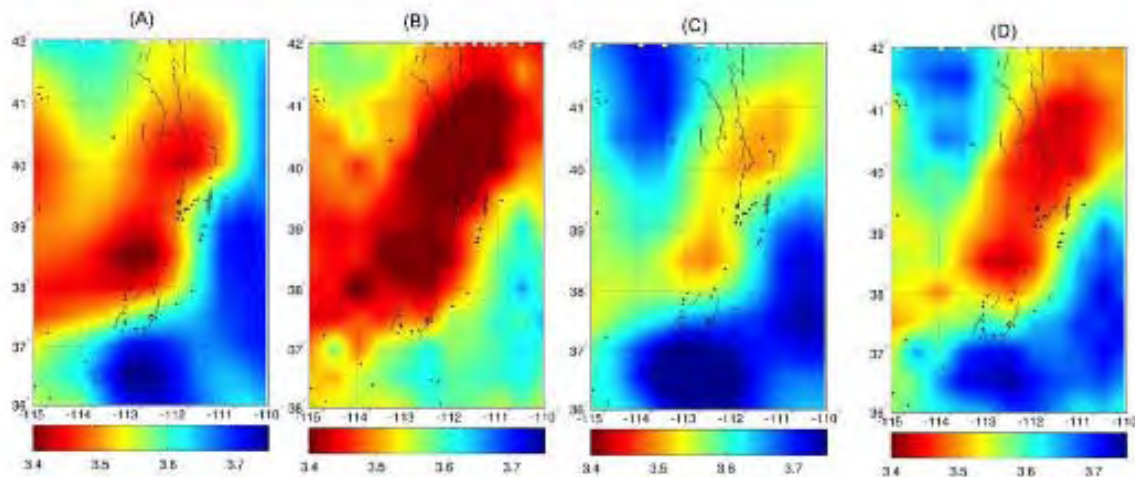

Figure 6. Shear-wave velocity model at a depth of 17 km obtained from (A) surface wave data, (B) surface and gravity data, (C) surface and travel time data, and (D) surface, gravity, and travel time data. (Velocity units: km/s).

Northwest China

Our final goal is to generate a 3D realistic and comprehensive model of the crustal and upper mantle seismic structure underneath northwest China, an area of prime importance for the nuclear explosion monitoring program. We have obtained a model from the joint inversion of surface waves dispersion measurements (Maceira et al., 2005), teleseismic P-wave receiver functions (Ammon et al., 2004), and gravity anomalies (Tapley et al., 2005). This model fits simultaneously all the data sets offering a compromise between fitting the three data sets (Figure 7).

We are now in the process of refining a new 3D model obtained by incorparating a fourth dataset in the inversion process. Body waves (P and S) travel times are gathered from the LANL Knowledge Database. Figure 8 shows preliminary results which are in good agreement with geological and tectonic knowledge of the area. Final results will be shown during the Monitoring Research Review in September.

Figure 7. Fit to the different datasets - P-wave receiver functions (top row), surface wave dispersion (middle row), gravity (bottom row) - from the inversion of surface waves and receiver functions (middle column) and from the joint inversion of the three datasets (right column).
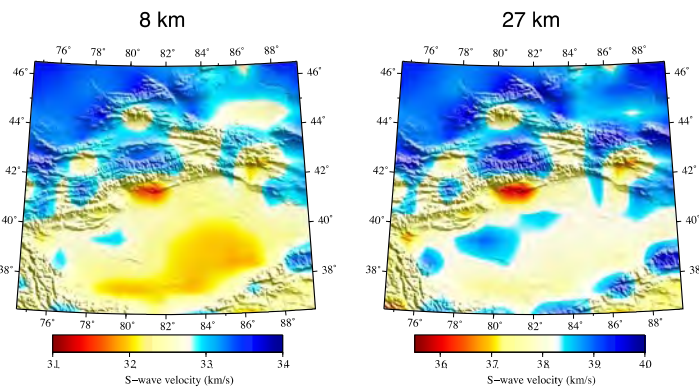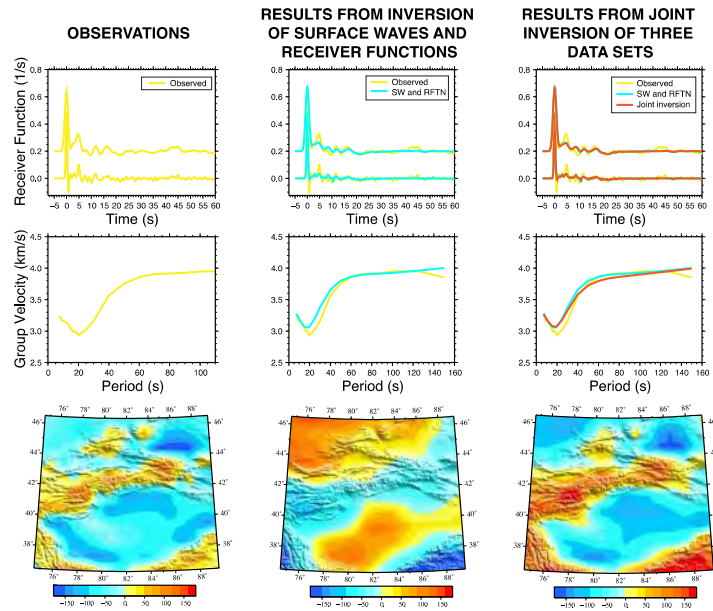

Figure 8. Vs model depth slices from joint inversion of body waves, surface waves, and gravity anomalies.
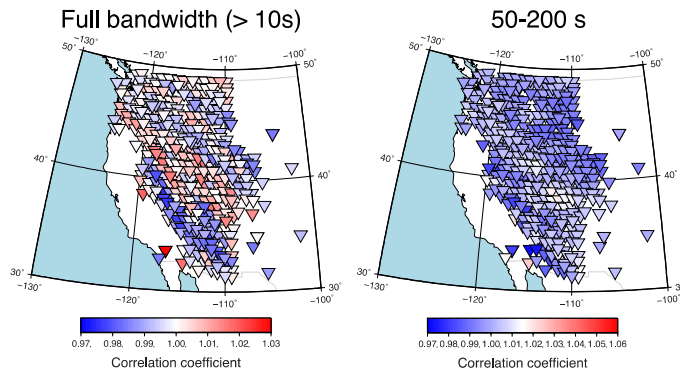
Model Validation

Figure 9. Cross correlation coefficient between synthetics computed from DNA model with finite-frequency and ray-theoretical approaches; (left) considering high frequencies, (right) only periods 50-200 s.

To address the need of near-regional to local nuclear explosion monitoring, several research institutions have been focused on inferring the best resolution possible images of the underground solid Earth. For the last three years, LANL has been developing and applying advanced multivariate inversion techniques to generate realistic and high-resolution 3D models of the seismic structure that satisfies numerous independent geophysical datasets. Our more complete models obtained by simultaneous joint inversion of disparate data sets produce better predictions and minimize the differences between observations and predictions. However, while our best current inversion techniques are providing 3D velocity models with the best resolution ever, they don't provide any absolute assessment of the model uncertainty. Theoretically, this will require testing the entire range of possible values for each parameter to get a complete "picture" of the solution space; in addition to questioning the fidelity of the imaging method (in this case, the seismic wave propagation scheme used to predict waveforms).

Geophysical model validation is typically done using resolution tests that assume the imaging theory used is accurate and thus only considers the impact of the data coverage for resolution. We are taking a more rigorous approach to model validation via full-waveform propagation. LANL High Performance Computing resources allow us to perform accurate 3D modeling of wave propagation through these models using the Spectral Element Method (SEM). This recently used in seismology technique makes no assumptions about the theory used to generate the models but require substantial computational resources. SEM is a particular case of continuous Galerkin method with optimized efficiency because of its use of high order and tensorized basis functions (Komatitsch and Tromp, 1999). It can handle very distorted elements (Oliveira & Seriani, 2011) imposed by complex geophysical models. The parallel implementation of SEM utilizes domain partition to partition the elements amongst the compute nodes. Current implementation incorporates 3D topography of seismic interfaces, anisotropy and attenuation.

We are currently and systematically computing the misfit between predicted and actually observed waveforms for the different Earth models generated in the project. Due to operational delays arising from the emergency LANL closure and incorrect shutdown of the HPC resources, we will present these results during the coming MRR. Figure 9 shows the idea of this model validation but with the DNA09-Berkeley model. The tests performed for this model and a moderate-sized event on the Pacific Northwest show no perceptible diffrerence between models obtained with two different imaging techniques (finite-frequency ray-theoretical) at intermediate periods. Differences star to appear, however, at higher frequencies.

CONCLUSIONS AND RECOMMENDATIONS

This is the last year of a three-year project to map the three-dimensional (3D) seismic structure of the crust and upper mantle using simultaneous joint inversion of surface wave dispersion, gravity, receiver function, and travel time observations. We have successfully accomplished our goal of developing an algorithm and corresponding computer codes for advanced multivariate inversion for Earth structure. We have dealt with multiple challenges of multivariate approaches such as relationship between independent variables in the inversion scheme and relative weighting of disparate datasets. We have also learned that besides enhancing resolution at short wavelengths, use of filtered gravity anomalies may help distinguish between anomalies at different depths. We are now refining and validating our 3D models for different areas around the globe. Our more rigorous approach to model validation via full-waveform propagation will, in the near-future, allow us to quantify model uncertainties and map them into the uncertainty in seismic source parameters.

REFERENCES

Ammon, C. J., W. Sevilla, R. B. Herrmann, and G. E. Randall (2004). Systematic inversion of receiver functions and surface wave dispersion for crustal structure in central Asia, in *Proceedings of the 26th Seismic Research Review: Trends in Nuclear Explosion Monitoring*, LA-UR-04-5801, Vol.1, pp. 29–38.

Bastow, I.D., G.W. Stuart, J.-M. Kendall, C. Ebinger (2005). Upper-mantle seismic structure in a region of incipient continental breakup: northern Ethiopian rift, *Geophs. J. Int.,* 162: 479–493.

Benoit, M. H., A. A. Nyblade, J. C. VanDecar (2006). Upper mantle P-wave speed variations beneath Ethiopia and the origin of the Afar hotspot, *Geology*, 34: 329–332.

Beutel, E., J. van Wijk, C. Ebinger, D. Keir, A. Agostini (2010). Formation and stability of magmatic segments in the Main Ethiopian and Afar rifts, *Earth Planet. Sci. Lett*. 293: 225–235.

Ebinger C. J., N.H. Sleep (2001). Cenozoic magmatism throughout east Africa resulting from impact of a single plume, *Nature*, 395: 788–791.

Ebinger, C. J. (1989). Tectonic development of the western branch of the East African rift system, *Geol. Soc. Am. Bull.* 101: 885–903.

Huang, Z., W. Su, Y. Peng, Y. Zheng, and H. Li (2003). Rayleigh wave tomography of China and adjacent regions, *J. Geophys. Res*. 108(B2): 2073, doi:10.1029/2001JB001696.

Julià, J., C. J. Ammon, R. B. Herrmann, and A. M. Correig (2000). Joint inversion of receiver function and surface wave dispersion observations, *Geophys. J. Int*. 143: 99–112.

Julià, J., C. J. Ammon, and A. A. Nyblade (2005). Evidence for mafic lower crust in Tanzania, East Africa, from joint inversion of receiver functions and Rayleigh wave dispersion velocities, *Geophys. J. Int.* 162: 555–569.

Keranen, K. M., S. L. Klemperer, J. F. Lawrence, J. Julia_, A. A. Nyblade (2009). Low lower crustal velocity across Ethiopia: Is the Main Ethiopian Rift a narrow rift in a hot craton?, *Geochemistry, Geophysics, Geosystems*, 10: 1–21.

Knox, R.P., A.A. Nyblade, C.A. Langston (1998). Upper mantle S velocities beneath Afar and western Saudi Arabia from Rayleigh wave dispersion, *Geophys. Res. Lett.* 25: 4233–4236.

Komatitsch, D., and J. Tromp (1999). Introduction to the spectral-element method for 3-D seismic wave propagation, *Geophys. J. Int.,* 139: (3), 806–822, doi: 10.1046/j.1365- 246x.1999.00967.x

Lebedev, S., and R.D. Van der Hilst (2008). Global upper-mantle tomography with the automated multimode surface and *S* waveforms, *Geophys. J. Int*., 173: 505–518.

Lees, J. M., and J. C. VanDecar (1991). Seismic tomography constrained by Bouguer gravity anomalies: Applications in western Washington, *Pure and Appl. Geophys*. 135: 31–52.

Maceira, M. and C. J. Ammon (2009). Joint inversion of surface wave velocity and gravity observations and its application to Central Asian basins shear velocity structure, *J. Geophys. Res*. 114: B02314, doi:10.1029/2007JB005157.

Maceira, M., C. Rowe, H. Zhang, R. Modrak, M. Begnaud, L. Steck, G. Randall, and X. Yang (2009). Advanced Multivariate Inversion Techniques for High Resolution 3D Geophysical Modeling, in *Proceedings of the 31st Monitoring Research Review: Ground-Based Nuclear Explosion Monitoring Technologies*, LA-UR-09-05276, Vol. 1, pp. 111–120.

Modrak, R.T., M. Maceira, J. Van Wijk, and M.E. Pasyanos (2011). Tomography of East Africa and analysis of rift structure through joint inversion of dispersion and gravity data, *Earth Planet. Sci. Lett.*., in review.

Nyblade, A. A., R. A. Brazier (2002). Precambrian lithospheric controls on the development of the East Africa rift system, *Geology*, 30: 755–758.

Nyblade, A.A., T.J. Owens, H. Gurrola, J. Ritsema, C.A. Langston (2000). Seismic evidence for a deep upper mantle thermal anomaly beneath east Africa, *Geology*, 28: 599–602.

Oliveira, S.P., and G. Seriani (2011). Effect of Element distortion on the numerical dispersion of spectral element methods, *Commun. Comput. Phys*., 9:4, 37–958.

Pasyanos, M. E., and A. A. Nyblade (2007). A top to bottom lithospheric study of Africa and Arabia, *Tectonophys.*, 444, 27–44.

Prodehl, C., et al. (1997). The KRISP 94 lithospheric investigation of southern Kenya- the experiments and their main results, *Tectonophysics*, 278, 121–147.

Ritsema, J., H. van Heijst (2000). New seismic model of the upper mantle beneath Africa, *Geology*, 28: 63–66.

Ritzwoller, M.H., and A.L. Levshin (1998). Eurasian surface wave tomography: Group velocities, *J.Geophys. Res.*, 103: 4839 – 4878.

Rogers, N., R. Macdonald, J.G. Fitton, R. George, M. Smith, B. Barreiro (2000). Two mantle plumes beneath the East African rift system: Sr, Nd and Pb isotope evidence from Kenya Rift basalts, *Earth Planet. Sci. Lett*. 176: 387–400.

Simiyu, S. M., G. R. Keller (1997). An integrated analysis of lithospheric structure across the East Africa plateau based on gravity anomalies and recent seismic studies, *Tectonophysics*, 278, 291–313.

Tapley, B. D., S. Bettadpur, J. C. Ries, P. F. Thompson, M. M. Watkins (2005). GRACE measurements of mass variability in the Earth system, *Science*, 305, 503–505.

Tessema, A., L. A. G. Antoine (2004). Processing and interpretation of the gravity field of the East African Rift: Implication for crustal extension, *Tectonophysics*, 394: 87–110.

Tiberi, C., M. Diament, J. Déverchère, C. Petit-Mariani, V. Mikhailov, S. Tikhhotsky, U. Achauer (2003). Deep structure of the Baikal rift zone revealed by joint inversion of gravity and seismology, *J. Geophys. Res*., 108, No. B3, 2133, doi:10.1029/2002JB001880.

Tromp J., C. Tape, Q. Liu (2005). Seismic tomography, adjoint methods, time reversal and bananadoughnut kernels, *Geophys. J. Int.* 160: 195–216.

Weeraratne, D. S., D. W. Forsyth, K. M. Fischer (2003). Evidence for an upper mantle plume beneath the Tanzanian craton from Rayleigh wave tomography, *J. Geophys. Res*. 108: No. B9, 2427, doi:10.1029/2002JB002273.

Wessel, P., W. H. F. Smith (1995). New version of the Generic Mapping Tools released, EOS Trans. AGU, 76: 329.

Yang, Y., Y. Zheng, and M.H. Ritzwoller (2010). Rayleigh wave phase velocity maps in Tibet and the surrounding regions from ambient seismic noise tomography, *Geochem., Geophys., Geosys.*, 11. Q08010.

Yang, Y., M. H. Ritzwoller, F.-C. Lin, M. P. Moschetti, and N. M. Shapiro (2008). Structure of the crust and uppermost mantle beneath the western United States revealed by ambient noise and earthquake tomography, *J. Geophys. Res*., 113: B12310, doi:10.1029/2008JB005833.

Yao, H., R.D. Van der Hilst, J-P. Montagner (2010). Heterogeneity and anisotropy of the lithosphere of SE Tibet from surface wave array analysis, *Geophys. J. Res.*, doi:10.1029/2009JB007142.

Yi, G., H. Yao, J. Zhu, R.D.Van der Hilst (2008). Rayleigh-wave phase velocity distribution in China continent and its adjacent regions, *Chinese J. Geophys.,* Vol.52, No. 2: 402–411.

Zeyen, H., U. Achauer (1997). Joint inversion of teleseismic delay times and gravity anomaly data for regional structures, in: K. Fuchs (ed.), *Upper Mantle Heterogeneities from Active and Passive Seismology*, Kluwer Academic Publishers, Dordrecht, 155–169.

Zhang, H., and C. Thurber (2006). Development and applications of double-difference tomography, *Pure and Applied Geophys.*, 163: 373–403, doi:10.1007/s00024-005-0021-y.

Zhang, H., and C. H. Thurber (2003). Double-Difference Tomography: The Method and Its Application to the Hayward Fault, California, *Bull. Seismol. Soc. Am.* 93: 1875–1889.

Zhao L., and T.H. Jordan (2006). Structural sensitivities of finite-frequency seismic waves: a full-wave approach, *Geophys. J. Int.* 165: 981–990.

Zheng, S., X. Sun, X. Song, Y. Yang, and M.H. Ritzwoller (2008). Surface wave tomography of China from ambient seismic noise correlation, *Geochem. Geophys. Geosyst.,* 9, Q05020, doi:10.1029/2008GC001981.